Journal of Coordination Chemistry

ISSN: (Print) (Online) Journal homepage: https://www.tandfonline.com/loi/gcoo20

On the synthesis and characterization of two different titanium-based supramolecular structures of identical stoichiometry

Ryan J. Bujol, Frank R. Fronczek & Noémie Elgrishi

To cite this article: Ryan J. Bujol, Frank R. Fronczek & Noémie Elgrishi (2022) On the synthesis and characterization of two different titanium-based supramolecular structures of identical stoichiometry, Journal of Coordination Chemistry, 75:11-14, 1768-1780, DOI: 10.1080/00958972.2022.2109149

To link to this article: https://doi.org/10.1080/00958972.2022.2109149

JOURNAL OF COORDINATION CHEMISTRY
2022, VOL. 75, NOS. 11–14, 1768–1780
https://doi.org/10.1080/00958972.2022.2109149

On the synthesis and characterization of two different titanium-based supramolecular structures of identical stoichiometry

Ryan J. Bujol, Frank R. Fronczek and Noémie Elgrishi

Department of Chemistry, Louisiana State University, Baton Rouge, LA, USA

ABSTRACT

Self-assembled supramolecular coordination complexes can take on a wide range of three-dimensional architectures with varying ratios of metal-to-ligand. Control over which architecture will be adopted can be difficult to maintain, as many may form from the starting materials and conditions present. Characterizing the resulting architectures formed can be challenging, in particular when discerning between lower or higher ordered structures of identical stoichiometry. Here we report the synthesis and characterization of a Ti_2L_3 football-like or pill-shaped capsule, unexpectedly formed from attempts to synthesize variations on a Ti_4L_6 tetrahedron. The two anionic cores are formed from identical stoichiometric ratios of organic linkers and metal nodes. The high symmetry of the structures, and identical m/z ratios, posed characterization challenges. Crystallization was the only method that allowed for precise structural determination. In the presence of appropriate counter ion guests, the Ti_2L_3 capsule converts into the Ti_4L_6 tetrahedron at elevated temperatures over several days.

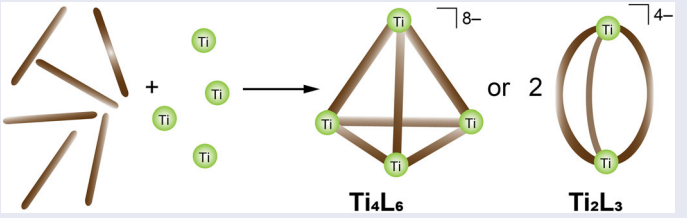

ARTICLE HISTORY
Received 3 May 2022
Accepted 28 July 2022

KEYWORDS
Cage; capsule; nanocontainer; titanium; M_2L_3; M_4L_6; interconversion

1. Introduction

Molecular metallocages continue to garner interest for their potential use as reaction vessels, drug delivery platforms, or as sequestering agents [1–4]. Molecular metallocages are porous polyhedral structures typically consisting of metal nodes at the vertices bridged by polydentate organic ligands. A variety of shapes, mostly Platonic solids,

CONTACT Noémie Elgrishi noemie@lsu.edu Department of Chemistry, Louisiana State University, 232 Choppin Hall, Baton Rouge, LA 70803, USA

Supplemental data for this article is available online at https://doi.org/10.1080/00958972.2022.2109149.

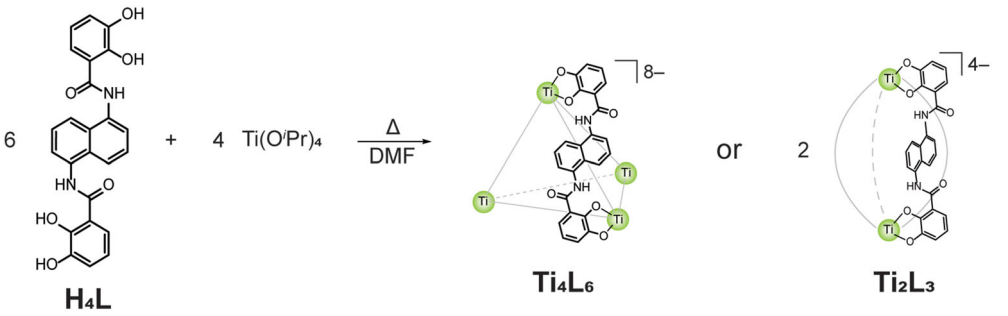

Scheme 1. Overview of the structure of H_4L ligand and of the stoichiometry of the Ti_4L_6 tetrahedron and the unexpected Ti_2L_3 capsule. The NEt_4^+ counter ions, introduced during synthesis as NEt_4Cl, are not shown for clarity. Only one ligand is shown in each structure for clarity. The Ti_4L_6 structure contains a total of six ligands arranged along each edge of the tetrahedron (grey lines). The Ti_2L_3 structure contains a total of three ligands (grey lines).

can be obtained from subcomponent self-assembly of predesigned organic linkers coordinating to metal centers depending on the nature and ratios of the metal salts and organic ligand used. These cages feature an internal void, which allows for confinement of appropriately sized molecules within the cavities, or host-guest chemistry [3, 5]. Due to their propensity for encapsulating guests, cages are sometimes called nano-capsules, porous coordination cages, nano-containers, or molecular flasks, among other terms [6, 7]. Host-guest chemistry within the confinement of the pores of supramolecular objects is receiving increasing attention due to the ability of the hosts to provide cavities with tailored properties, different from the surrounding solvent. These properties have been used to shield and stabilize highly reactive compounds or catalytic intermediates [8–10], to promote unexpected reactivity [11–13], or to solubilize drugs [14–18].

The underlying self-assembly of organic ligands and metal ions into supramolecular architectures is well studied, with structures obtained ranging from small helicates to tetrahedra, octahedra, and even large balls, among others [4, 19–21]. The structures are generally labeled with the notation M_xL_y where M is the metal, L is the ligand, and x and y are the corresponding stoichiometric ratios. Which architecture is formed depends on a multitude of parameters, including factors related to ligand choice (e.g. shape, denticity, bite angles, functional groups, and rigidity), to node choice (metal identity, oxidation state), or to the choice of reaction conditions (e.g. solvent and temperature). All these parameters generally allow for a level of predictability and control over preferred structures [3, 22–24]. However, it is not uncommon for a reaction to yield multiple products varying by metal-to-ligand ratios leading to multiple architectures and orientations [25–31]. More rarely, it is possible to obtain different structures of identical stoichiometric ratios [32–39]. Such situations lead to special challenges in correctly identifying the products as the metal-to-ligand ratios are identical and the ligand symmetries are often maintained. Assigning structures from routine characterization techniques becomes challenging, as properties of these other complexes may be identical to the expected architecture. Herein, we report a new Ti_2L_3 structure, shaped like an oblong pill and referred to as capsule based on its shape,

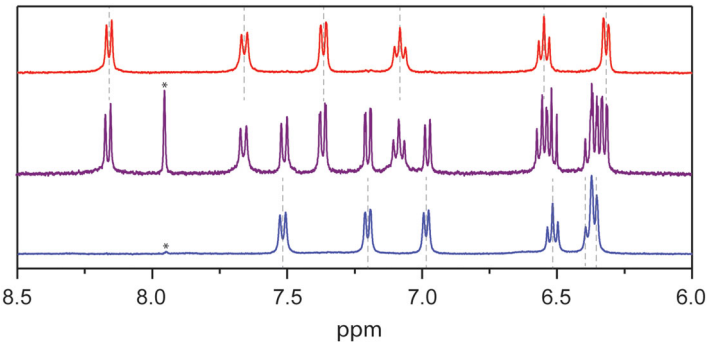

Figure 1. Aromatic ^{1}H NMR profiles of isolated $(NEt_4)_8[Ti_4L_6]$ (top, red) and $(NBu_4)_4[Ti_2L_3]$ (bottom, blue), as well as an example of product mixture obtained before purification (middle, purple) in DMSO-d_6. A DMF solvent residual peak, identified by a star symbol can be observed at 7.95 ppm. Data collected on a 400 MHz instrument.

unexpectedly obtained from conditions generally used for the formation of a Ti_4L_6 tetrahedron (Scheme 1).

2. Results and discussion

2.1. Ti_2L_3 structure characterization

Raymond and coworkers reported a Ti_4L_6 porous tetrahedral structure, where four Ti(IV) metal nodes are at the corners of a tetrahedron, linked by six ligands "L" along the edges of the tetrahedron [40]. The structure is charged −8, and is reported with NEt_4^+ counter ions including one NEt_4^+ ion encapsulated in the cavity of the tetrahedron [40]. The tetrahedron can be formed from a dicatecholamidonaphthalene ligand (= H_4L) and a titanium salt in the presence of a base (Scheme 1) [40]. This cage features a naphthalene ligand core and dicatecholamido binding motifs, which act as the coordinating pocket for the titanium ions. This ligand has been designed to obtain M_4L_6 type structures exclusively and prevent the formation of lower order helicate-type structures [20, 41]. Varying the metal salt has been a strategy to obtain a range of similar tetrahedral structures of general form M_4L_6 [40–43]. In particular, using M = Ga(III) was reported to yield a similar tetrahedral Ga_4L_6 cage, charged −12, with again NEt_4^+ counter ions including one NEt_4^+ ion encapsulated in the cavity of the tetrahedron [41]. This particular cage exhibits excellent host-guest properties when synthesized with alkali metal counter ions, which do not reside within the cavity because of their smaller size [41]. The Ga_4L_6 cage has been reported to encapsulate a wide scope of molecules, both organic and organometallic [44]. The cavity of the cage has also served as a stabilization pocket for reaction intermediates, and unexpected reactivity has been reported such as electrocyclization and proton mediated catalysis [45–47]. Given the prior reports of the excellent host-guest properties of this family of supramolecular objects, synthesis of the related Ti_4L_6 structures with alkali metal counter ions would be beneficial.

Formation of the Ti_4L_6 tetrahedral structure requires high temperatures, and *in situ* DMF solvent degradation has been proposed to provide the required base [40]. As

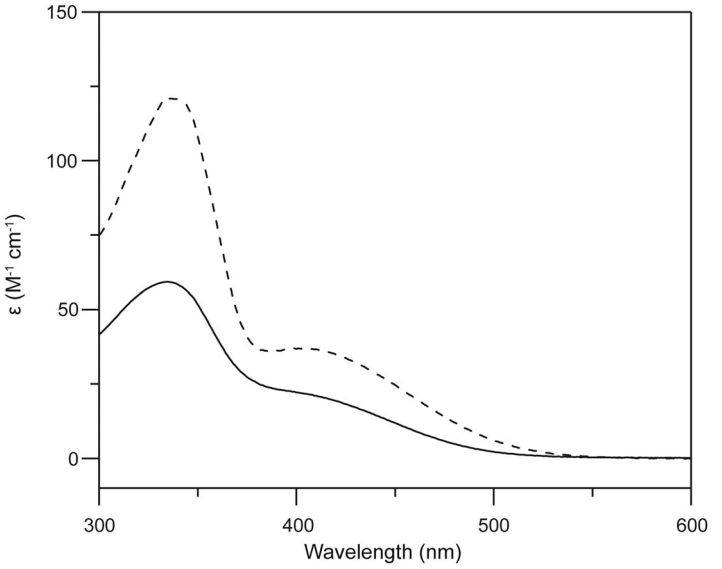

Figure 2. Extinction coefficients versus wavelength of $K_4[Ti_2L_3]$ (solid line) and $(NEt_4)_8[Ti_4L_6]$ (dashed line) in MeOH.

synthesized, following literature precedent, the Ti_4L_6 cage contains one encapsulated NEt_4^+ counter ion and is typically obtained in low yields [40]. Our attempts at synthesizing the Ti_4L_6 cage with other alkylammonium counter ions, or alkali metal counter ions, have so far not been successful. However, these attempts often yielded the same materials with a single set of aromatic ^{1}H NMR peaks, at different resonances than for free ligand, implying the formation of a single highly symmetric product (Figure 1, bottom). Moreover, characterization of the reaction mixture during Ti_4L_6 synthesis in the presence of NEt_4^+ ions before purification showed the presence of two sets of resonances corresponding to the ligand (Figure 1, middle). One set was attributed to the expected Ti_4L_6 tetrahedron based on comparison with an independently synthesized sample (Figure 1, top), and the other matched the resonances for the new species observed in reactions using different counter ions (Figure 1, bottom and middle).

First identified through ^{1}H NMR spectroscopy, the structure of the new product was only established as of the form Ti_2L_3 through single crystal X-ray crystallography (*vide infra*) and is referred to as Ti_2L_3 moving forward. The attributions of ^{1}H NMR signals to the new Ti_2L_3 structure were confirmed after authentic samples were isolated and purified. Characterization using ^{1}H NMR spectroscopy data showed that both the Ti_2L_3 and Ti_4L_6 structures are highly symmetric, exhibiting only six aromatic peaks for ligand protons, plus a broad N-H resonance (see Supplementary Data). Two of the resonances overlap at 6.36 ppm in the Ti_2L_3 structure (Figure 1, bottom). While the observed ^{1}H NMR peak shifts are distinctive, ^{1}H NMR alone was not sufficient in establishing the structure. ^{13}C NMR spectroscopy data were also collected, and simply confirmed that the expected ligands were present. DOSY experiments did yield significantly different diffusion coefficients for the two species, with D_0 values of 8.54×10^{-7} cm^2 s^{-1} measured for the Ti_4L_6 cage and 1.5×10^{-6} cm^2 s^{-1} for the Ti_2L_3 structure. The significantly larger diffusion coefficient for the Ti_2L_3 structure is in agreement with the structural

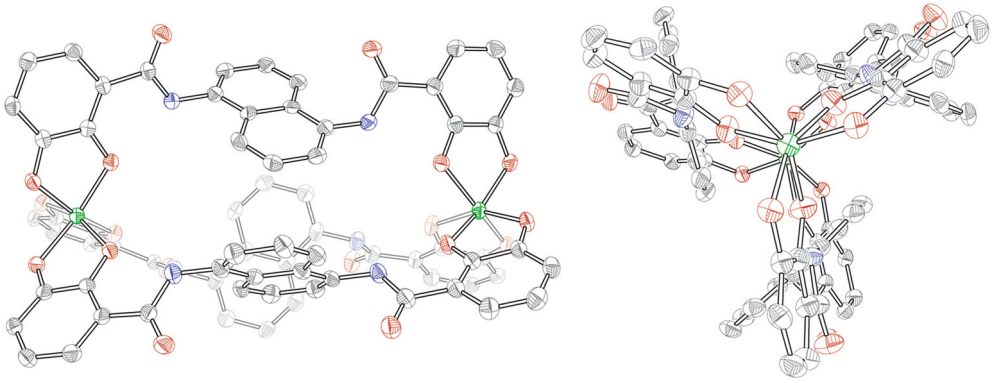

Figure 3. Side (left) and top (right) views of the single-crystal structure of Ti_2L_3, formally obtained with mixed counter ions as $K(NBu_4)_3[Ti_2L_3]$, with ellipsoids drawn at 50% probability with the colors: C gray, N blue, O red, Ti green. Counter ions, hydrogens, and solvent molecules deleted for clarity. Back ligand is shaded in the side-view to help visualize the structure.

assignment, though cannot provide structure determination on its own. Other common characterization techniques are also weak in determining a new structure made of identical ligands and metals in identical stoichiometric ratios (e.g. elemental analysis and mass spectrometry). UV–vis spectra of the two species (Figures S11 and S12) show absorbance features at 335 nm and 404 nm in methanol for the Ti_4L_6 cage and at 334 nm with a shoulder around 405 nm in methanol for the Ti_2L_3 capsule. While the extinction coefficients are significantly different, about twice as large for the Ti_4L_6 cage, these could be determined only after structural identity was established (Figure 2).

The structure was established through single crystal X-ray crystallography. Crystals of the new material were grown with mixed NBu_4^+ and potassium cations, revealing the structure as a Ti_2L_3 oblong pill-shaped capsule, resembling an American football or rugby ball (Figures 3, S13–S15). This was quite unexpected, as the ligand had been designed specifically to avoid the formation of lower order structures of this type [41]. The H_4L ligand used is reported to prevent the formation of lower ordered structures due to an offset of the catechol moieties allowing for C_2 symmetry. The C_2 symmetry of the ligand promotes binding of the ligand to two metals on opposite sides, which is expected to have the ideal geometry to lead to formation of a Ti_4L_6 tetrahedral cage, disallowing the formation of helicate type structures [20, 41]. However, as evidenced by the obtained crystal structures of the Ti_2L_3 capsule, the C_2 symmetry of the ligand is not always maintained and at least one pair of catechols are seen binding to two metals on the same side. This is in contrast with the binding motifs observed in Ti_4L_6 cages. Additionally, oxygens in both amido groups on a ligand point above the plane of the ligand's naphthalene core, causing a twist in the angle of the catechol benzene ring, enforcing the odd binding behavior. This is not seen in the reported crystal structure of Ti_4L_6, which shows the typical offset catechol binding with planar ligands [48]. The Ti_2L_3 structure exhibits a Ti-Ti distance of 12.6 Å, which is comparable with the average Ti-Ti distance in Ti_4L_6 of 12.81 Å as well as the 12.8 Å reported for the related Fe_4L_6 structure [41]. In a second crystal structure obtained, more

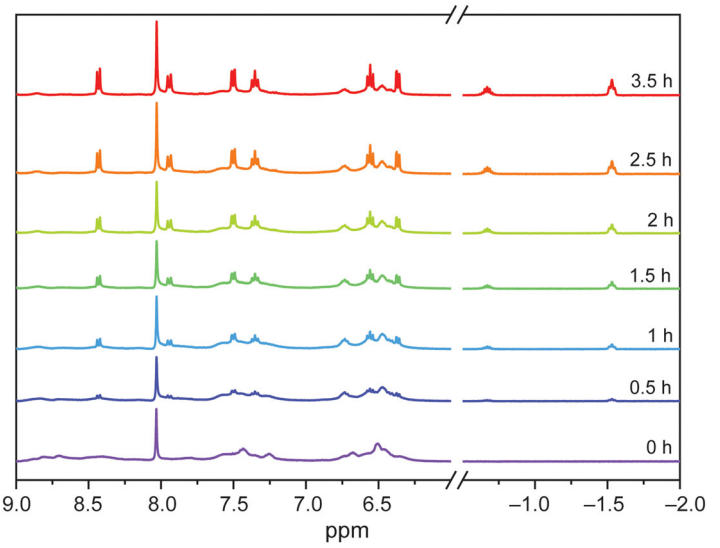

Figure 4. Growth of Ti_4L_6 peaks at 140 °C during NMR scale synthesis in DMF-d_7. NEt_4Cl, H_4L ligand, and $Ti(O^iPr)_4$ mixed air free in a 4:3:2 ratio. Only the aromatic region and the region expected to contain the encapsulated NEt_4^+ are shown for clarity. Data collected in a high-pressure NMR tube on a 400 MHz instrument.

disordered and with only potassium counter cations, a smaller Ti-Ti distance of 11.5 Å is observed (Figure S15). This structure also exhibited different ligand orientations, with more of a helicate structure as seen in the views down the Ti-Ti axes (Figure 3 compared to Figure S16). Both crystal structures emphasize the lack of symmetry of the ligands in the solid state. Structures in which two metal centers are bound by three ligands are not rare. The metal-to-metal distances vary depending on the choice of metals and ligands. In these structures, it is often possible to observe a regular twist of the ligands from one metal center to the other, which gives rise to the name helicate [20]. This helical motif is not observed in the crystal structure of the Ti_2L_3 capsules in Figure 3 with tetrabutylammonium counter ions (Figure 3), though it is partially present in the disordered structure with only K^+ counter ions (Figure S16).

2.2. Factors influencing Ti_4L_6 or Ti_2L_3 formation

Once the Ti_2L_3 structure was identified, it was observed to form with a variety of counter ions. It was found that the Ti_2L_3 core, charged −4, can be synthesized as NR_4^+ salts (R = Et, Pr, Bu), as confirmed by ^1H NMR spectroscopic data. It can also form as the K^+ salt when an external base such as KOH is added to the reaction instead of relying on the solvent-degradation base formation. High heat did not appear to be as critical to the formation of the Ti_2L_3 structure in the presence of an external base such as KOH, suggesting it is a kinetic product. Ti_2L_3 was also found to be air stable, contrary to samples of the Ti_4L_6 cage.

Conditions favoring the formation of one product over another were studied. It was seen that during the synthesis of the Ti_4L_6 cage, using DMF degradation as the base and NEt_4Cl as the counter ion source, the Ti_2L_3 structure formed in small amounts.

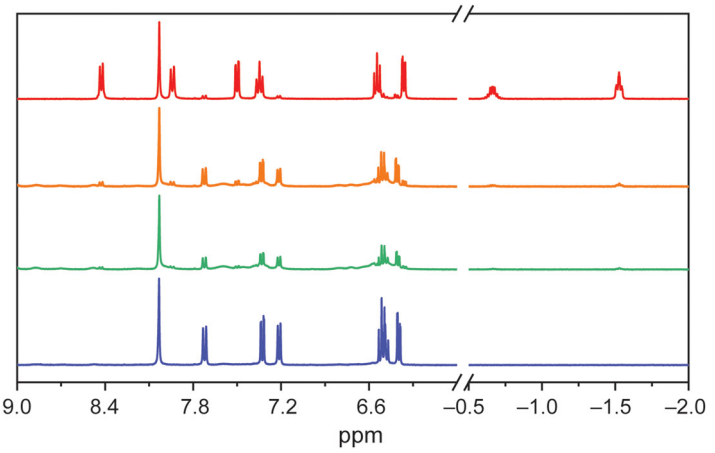

Figure 5. Conversion of $K_4[Ti_2L_3]$ capsule into Ti_4L_6 in DMF-d_7 in the presence of excess NEt_4Cl. Little growth was seen from the initial (bottom, blue) spectrum after 5 days of heating at 140 °C (green). Heating at 150 °C for one day (orange) yielded some conversion before complete conversion was observed the following day (red, top). Data collected in a high-pressure NMR tube on a 400 MHz instrument.

The subsequent MeOH wash purification step removed the formed Ti_2L_3 structure, leaving the pure Ti_4L_6 cage as the isolated product. However, if NEt_4OH is added as both base and counter ion source in the reaction mixture, only a small amount of Ti_4L_6 cage is formed at 120 °C, and the major product is the Ti_2L_3 capsule. The base formed through the degradation of DMF, or perhaps the higher temperatures required to induce base formation, appears critical in obtaining the Ti_4L_6 cage. This is surprising as that is not the case for the related Ga_4L_6 structure. Since the DMF degradation is proposed to be triggered by high heat, it suggests that the Ti_4L_6 structure is the thermodynamic product while the Ti_2L_3 structure is a kinetic product.

To further probe this kinetic/thermodynamic product relationship, Ti_4L_6 synthesis was set up in a high-pressure NMR tube and the evolution of the reaction mixture tracked over time as heat was applied (Figure 4). On first approximation it would be expected that, if Ti_2L_3 were a kinetic product, it would form quickly in the NMR sample, followed by slow transformation to the cage as the thermodynamic product with heat over time. However, this was not observed. Instead, exclusive formation of the Ti_4L_6 cage was seen as heat was applied, in amounts increasing over time (Figure 4). The presence of the cage is easily tracked by the two highly shielded signals corresponding to the encapsulated NEt_4^+ counter ions at negative ppm shifts. Small Ti_2L_3 capsule peaks are observed coming out of the baseline only in later traces, once the baseline is clear enough for them to be observable. Since temperature-induced DMF degradation is proposed to be the source of the base in solution required to initiate the reaction, it is possible that by the time the base is formed, the energy required to form the Ti_4L_6 cage product is already present. This would explain the lack of strong Ti_2L_3 resonances throughout the reaction.

To further investigate this system, an attempt to directly convert the Ti_2L_3 capsule into the Ti_4L_6 cage was set up in an NMR tube in DMF-d_7 and the reaction was

monitored over time (Figure 5). The potassium salt of the capsule $K_4[Ti_2L_3]$ was heated in the presence of NEt_4Cl, to provide NEt_4^+ as guest for the cage. This also allowed a convenient handle to observe the encapsulated NEt_4^+ peak at negative ppm values. When holding the temperature at 140 °C, the temperature used during the synthesis of Ti_4L_6, minimal transformation occurred over 5 days. However, once the temperature was increased to 150 °C, much quicker transformations were seen, with nearly complete conversion from Ti_2L_3 to Ti_4L_6 over 48 h. This supports the claim that Ti_2L_3 is a kinetic product, which converts into the thermodynamic product Ti_4L_6 with enough energy.

When comparing the behavior of the Ga_4L_6 and Ti_4L_6 systems, it is striking that high temperatures are required for the Ti_4L_6 cage but not for the Ga_4L_6 cage. It is also noteworthy that the Ti_4L_6 synthesis occurs only when using high temperatures close to the boiling point of DMF, and that at 140 °C only DMF-decomposition as a base was successful in forming Ti_4L_6. This is in contrast with the Ga_4L_6 cage which forms at lower temperatures, using KOH as a base. Strikingly, the Ga_2L_3 capsule analogous to the Ti_2L_3 capsule reported here has never been observed to date. The ligand used had been specifically designed to disallow the formation of M_2L_3 type structures, and none had been reported previously [20, 41]. These observations could be explained by the greater lability of the Ga-O bonds compared to Ti–O bonds, which allows the Ga system to self-assemble and self-correct any binding "mistakes." The Ti system on the other hand requires more energy to break the Ti–O bonds for corrections, meaning that higher temperatures are required to reach the thermodynamic sink. It is possible that if Ga_2L_3 capsule transiently formed during synthesis, the lability of the Ga–O bonds would lead to the thermodynamic product Ga_4L_6 being eventually reached through self-correction during the self-assembly reaction.

3. Experimental

3.1. General considerations

Reagents and solvents used were obtained from commercial sources and used without further purification unless otherwise stated. Methanol (ACS grade, VWR Chemicals BDH®), diethyl ether (≥99.0% GR ACS, MilliporeSigma), potassium hydroxide (≥85%, VWR Chemicals BDH®), tetraisopropyl orthotitanate (TCI), tetraethylammonium chloride (96%, Alfa Aesar), tetrapropylammonium bromide (98%, Acros Organics), and tetrabutylammonium bromide (99%, Strem) were used as received. Dimethylformamide (99.8%, DriSolv® Supelco® MilliporeSigma), DMF-d_7 (D 99.5%, Acros Organics), and DMSO-d_6 (D > 99.8%, MagniSolv™ MilliporeSigma) were stored over 3 Å activated sieves. Reactions under inert atmosphere were performed inside an oxygen- and water-free Unilab Pro SP MBRAUN glovebox unless specified. NMR spectra were collected with a 400 or 500 MHz Bruker spectrometer. NMR shifts are reported as δ in ppm and referenced to the corresponding solvent residual peak [49]. NMR scale reactions were performed in regular J-Young tubes or high pressure NMR tubes from Wilmad-LabGlass. UV–vis data were recorded using an Agilent Cary 5000 UV–vis-NIR spectrophotometer. Crystallographic data were collected at T = 90 K on a Bruker *APEX*-

II DUO diffractometer equipped with Cu microfocus source. H_4L was synthesized according to literature procedures and ^1H NMR characterization data matches the literature (Figure S10) [41]. All syntheses were set up in an inert atmosphere glovebox. The workup was done in an inert atmosphere glovebox unless otherwise noted.

3.2. Synthesis of $K_4[Ti_2L_3]$

The ligand H_4L (199.7 mg, 0.464 mmol) was dissolved in 25 mL of DMF and transferred to a Schlenk flask. KOH was dissolved in MeOH to yield a 423.1 mM solution and 2.19 mL was added to the solution of ligand, turning the colorless solution light yellow. To this, $Ti(O^iPr)_4$ (91.6 μL, 0.31 mmol) was added, immediately turning the solution bright orange. The flask was sealed and stirred for 5 days at 140 °C. The solvent was concentrated under vacuum to ~2 mL, producing a small amount of a white solid, which was removed by filtration. In a fume hood, ether was added to crash out an orange solid, which was collected by filtration. This solid was washed with 100 mL of a 5% MeOH in ether solution to remove excess DMF, before further drying under vacuum. 167.1 mg were collected (70% isolated yield). Crystals were grown by slow diffusion of diethyl ether in DMF solution of the product, yielding orange needles. ^1H NMR (500 MHz, DMSO-d_6) δ: 11.32 (s, 6H), 7.51 (d, 6H), 7.20 (d, 6H), 6.98 (d, 6H), 6.53 (t, 6H), 6.38 (m, 12H). ^{13}C NMR (500 MHz, DMSO-d_6) δ: 164.98, 160.47, 160.12, 133.73, 127.29, 124.42, 119.32, 117.70, 117.62, 116.16, 115.35, 112.81, 30.76. See Figures S1–S3. DOSY NMR: an average D_0 value of 1.5×10^{-6} cm^2 s^{-1} was calculated by using a Bruker pulse program with 2D sequence for diffusion measurement with stimulated echo and LED (longitudinal eddy current delay), bipolar gradient pulses for diffusion, and 2 spoil gradients.

3.3. Synthesis of $(NEt_4)_8[Ti_4L_6]$

Following literature precedents [40], H_4L (200 mg, 0.465 mmol) and NEt_4Cl (115.4 mg. 0.696 mmol) were dissolved in 65 mL of DMF and transferred to a Schlenk flask. To this, $Ti(O^iPr)_4$ (91.8 μL, 0.31 mmol) was added, turning the solution blood red. The flask was sealed and stirred for 5 days at 140 °C. During this time, the solution color lightened to an orange color. $NaHCO_3$ (50 mg) in 1 mL degassed water was added to the solution via a cannula. The solvent was removed under vacuum before the material was suspended in MeOH and filtered, followed by further MeOH washes. The MeOH washes remove any formed Ti_2L_3. The washed solid was collected and dried under vacuum (100.4 mg, 34% isolated yield). ^1H NMR (500 MHz, DMSO-d_6) δ: 11.77 (s, 12H), 8.17 (d, 12H), 7.66 (d, 12H), 7.37 (d, 12H), 7.09 (t, 12H), 6.56 (t, 12H), 6.33 (d, 12H), 3.07 (q, 56H), 1.06 (t, 84H), −0.93 (m, 8H), −1.78 (t, 12H). ^{13}C NMR (500 MHz, DMSO-d_6) δ: 164.83, 159.68, 159.62, 134.10, 125.60, 125.07, 118.18, 116.86, 116.62, 115.89, 115.08, 113.26, 51.35, 49.48, 6.98, 3.37. See Figures S4–S6. DOSY NMR: An average D_0 value of 8.54×10^{-7} cm^2 s^{-1} was calculated by using a Bruker pulse program with 2D sequence for diffusion measurement with stimulated echo and LED (longitudinal eddy current delay), bipolar gradient pulses for diffusion, and 2 spoil gradients.

3.4. Synthesis of $(NEt_4)_4[Ti_2L_3]$

Equimolar quantities of NEt_4Cl and KOH were combined in MeOH and mixed, precipitating KCl. This solution was filtered and diluted to 5 mL to obtain a 157.56 mM NEt_4OH stock solution. H_4L (30 mg, 0.0697 mmol) was dissolved in 10 mL of DMF and transferred to a Schlenk flask. To this, 0.9 mL of the NEt_4OH solution (0.142 mmol) was added with stirring, turning the colorless solution yellow. $Ti(O^iPr)_4$ (13.766 μL, 0.0465 mmol) was then added, turning the solution bright orange. The flask was sealed and stirred for 5 days at 120 °C. The solution was cooled and concentrated to a small volume under vacuum, before ether was added to precipitate an orange solid, which was collected by filtration. The solid was washed with ether and dried to yield 40 mg of solid. Using ^1H NMR integration, this solid is estimated to contain 90% of $(NEt_4)_4[Ti_2L_3]$ capsule, for an estimated overall reaction yield of 75%. Notably, this species was never able to be isolated as a single product, as a small amount of $(NEt_4)_8[Ti_4L_6]$ cage is formed alongside the Ti_2L_3 capsule (see Figure S7). ^1H NMR (400 MHz, DMF-d_7) δ: 11.61 (s, 6H), 7.72 (d, 6H), 7.32 (d, 6H), 7.21 (d, 6H), 6.48 (m, 12H), 6.36 (d, 6H), 3.35 (q), 1.25 (t).

3.5. Synthesis of $(NPr_4)_4[Ti_2L_3]$

Equimolar quantities of NPr_4Br and KOH were combined in MeOH and mixed, precipitating KBr. This solution was filtered and diluted to 5 mL to obtain a 152.2 mM NPr_4OH stock solution. H_4L (30 mg, 0.0697 mmol) was dissolved in DMF and transferred to a Schlenk flask. To this, 1 mL of the NPr_4OH stock solution (0.152 mmol) was added with stirring, turning the clear colorless solution light brown, and slightly cloudy. $Ti(O^iPr)_4$ (13.77 μL, 0.0465 mmol) was then added, turning the solution orange. The flask was sealed and stirred at 120 °C for 5 days. Once at temperature, the cloudiness dissipated. The solution was cooled and concentrated to a small volume under vacuum, before ether was added to precipitate an orange solid, which was collected by filtration. The solid was washed with ether and dried to yield 34 mg of solid (69% isolated yield). ^1H NMR (400 MHz, DMF-d_7) δ: 11.61 (s, 6H), 7.72 (d, 6H), 7.32 (d, 6H), 7.21 (d, 6H), 6.49 (m, 12H), 6.38 (d, 6H), 3.29 (m), 1.76 (sextet), 0.95 (t) (Figure S8).

3.6. Synthesis of $(NBu_4)_4[Ti_2L_3]$

Equimolar quantities of NBu_4Br and KOH were combined in MeOH and mixed, precipitating KBr. This solution was filtered and diluted to 5 mL to obtain a 191 mM NBu_4OH stock solution. H_4L (100.1 mg, 0.233 mmol) was dissolved in DMF and transferred to a Schlenk flask. To this, 2.427 mL of the NBu_4OH stock solution was added with stirring, turning the colorless solution pale yellow. $Ti(O^iPr)_4$ (45.89 μL, 0.0155 mmol) was then added, turning the solution blood red. The flask was sealed and stirred at 120 °C for 8 days. The solution turned from blood red to dark orange during this time. The solution was cooled and 25 mg of $NaHCO_3$ in 0.5 mL of degassed water were added to the solution via a cannula, though it was later determined that this step is not necessary. The solution was concentrated to a small volume under vacuum. In a fume hood, ether was added to precipitate an orange solid, which was collected by filtration. The

solid was washed with ether, followed by 10% MeOH in ether to yield 122 mg of dried solid (67% isolated yield). Crystals were grown in the presence of K^+ from KOH by slow diffusion of diethyl ether in DMF solution of the product, yielding tiny orange crystals. ^{1}H NMR (400 MHz, DMSO-d_6) δ: 11.32 (s, 6H), 7.51 (d, 6H), 7.20 (d, 6H), 6.98 (d, 6H), 6.51 (t, 6H), 6.36 (m, 12H), 3.12 (m, 36H), 1.52 (m, 32H), 1.28 (sextet, 32H), 0.91 (t, 48H) (Figure S9).

4. Conclusion

The unexpected formation of an American football or pill-shaped structure, called capsule due to its shape, of the general form Ti_2L_3 was reported, and the structure characterized. The new structure type forms using the same reagents in the same ratios as the expected larger order Ti_4L_6 cage previously reported. The formation of this new Ti_2L_3 structure was surprising as the highly studied ligand had been designed to exclusively form cages of the form M_4L_6 and prevent formation of lower order capsules [20, 41]. It is proposed that the low lability of the Ti-O bonds, compared to Ga-O, contribute to the unique observation of the M_2L_3 structure when M = Ti. The Ti_2L_3 structure forms readily and is obtained when using K^+, NEt_4^+, NPr_4^+, or NBu_4^+ counter ions. The Ti_4L_6 cage appears to be the thermodynamic product as it can be obtained from the Ti_2L_3 capsule in the presence of NEt_4^+ counter ions at high temperature. Characterization of the new lower order Ti_2L_3 structure was challenging due to the identical stoichiometric ratios of the Ti_2L_3 and Ti_4L_6 structures. This serves as a caution when developing new symmetric porous coordination structures, even when using highly established ligands. It also highlights the need for the development of enhanced methods for crystal growth and structural determination for supramolecular objects which are notoriously difficult to crystallize [50].

Acknowledgements

The authors thank Dr. Thomas Weldeghiorghis from the LSU Chemistry NMR Facility for help with DOSY experiments.

Disclosure statement

No potential conflict of interest was reported by the authors.

Funding

The authors acknowledge support from the National Science Foundation under award number 2046445 and from Louisiana State University startup funds. RJB thanks the Louisiana Board of Regents for partial fellowship support under award number LEQSF(17-22)-GF-03.

ORCID

Frank R. Fronczek http://orcid.org/0000-0001-5544-2779
Noémie Elgrishi http://orcid.org/0000-0001-9776-5031

References

[1] S.J. Dalgarno, N.P. Power, J.L. Atwood. *Coord. Chem. Rev.*, **252**, 825 (2008).
[2] H. Amouri, C. Desmarets, J. Moussa. *Chem. Rev.*, **112**, 2015 (2012).
[3] D. Zhang, T.K. Ronson, J.R. Nitschke. *ACC Chem. Res.*, **51**, 2423 (2018).
[4] Z. Wu, K. Zhou, A.V. Ivanov, M. Yusobov, F. Verpoort. *Coord. Chem. Rev.*, **353**, 180(2017).
[5] T.R. Cook, P.J. Stang. *Chem. Rev.*, **115**, 7001 (2015).
[6] M. Yoshizawa, J.K. Klosterman, M. Fujita. *Angew Chem. Int. Ed.*, **48**, 3418 (2009).
[7] M. Pattabiraman, A. Natarajan. *Photophysicochemical Processes Directed within Nano-Containers*, In Martínez-Martínez, V., López Arbeloa, F. (eds) Dyes and Photoactive Molecules in Microporous Systems. Structure and Bonding, vol 183. Springer, Cham. 321–369 (2020). https://doi.org/10.1007/430_2020_64.
[8] P. Mal, B. Breiner, K. Rissanen, J.R. Nitschke. *Science*, **324**, 1697 (2009).
[9] A. Galan, P. Ballester. *Chem. Soc. Rev.*, **45**, 1720 (2016).
[10] M.D. Bairagya, R.J. Bujol, N. Elgrishi. *Chem. Eur. J.*, **26**, 3991 (2020).
[11] M. Morimoto, S.M. Bierschenk, K.T. Xia, R.G. Bergman, K.N. Raymond, F.D. Toste. *Nat. Catal.*, **3**, 969 (2020).
[12] A.W. Kleij, J.N.H. Reek. *Chem. Eur. J.*, **12**, 4218(2006).
[13] K. Wang, J.H. Jordan, X.Y. Hu, L. Wang. *Angew. Chem. Int. Ed.*, **59**, 13712 (2020).
[14] J. Han, A.F.B. Räder, F. Reichart, B. Aikman, M.N. Wenzel, B. Woods, M. Weinmüller, B.S. Ludwig, S. Stürup, G.M.M. Groothuis, H.P. Permentier, R. Bischoff, H. Kessler, P. Horvatovich, A. Casini. *Bioconjug. Chem.*, **29**, 3856 (2018).
[15] J. Han, A. Schmidt, T. Zhang, H. Permentier, G.M.M. Groothuis, R. Bischoff, F.E. Kühn, P. Horvatovich, A. Casini. *Chem. Commun.*, **53**, 1405 (2017).
[16] J. Liu, T. Luo, Y. Xue, L. Mao, P.J. Stang, M. Wang. *Angew. Chem. Int. Ed.*, **60**, 5429 (2021).
[17] A. Süle, L. Szente, F. Csempesz. *J. Pharm. Sci.*, **98**, 484 (2009).
[18] C.Y. Zhu, M. Pan, C.Y. Su. *Isr. J. Chem.*, **59**, 209 (2019).
[19] H. Miyake, H. Tsukube. *Chem. Soc. Rev.*, **41**, 6977 (2012).
[20] M. Albrecht. *Eur. J. Inorg. Chem.*, **2020**, 2227 (2020).
[21] K. Su, M. Wu, D. Yuan, M. Hong. *Nat. Commun.*, **9**, 4941 (2018).
[22] R. Chakrabarty, P.S. Mukherjee, P.J. Stang. *Chem. Rev.*, **111**, 6810 (2011).
[23] A.E. Martín Díaz, J.E.M. Lewis. *Front. Chem.*, **9**, 706462 (2021). June 17 https://doi.org/10.3389/fchem.2021.706462.
[24] D. Zhang, Q. Gan, A.J. Plajer, R. Lavendomme, T.K. Ronson, Z. Lu, J.D. Jensen, B.W. Laursen, J.R. Nitschke. *J. Am. Chem. Soc.*, **144**, 1106 (2022).
[25] S. Hiraoka, K. Harano, M. Shiro, M. Shionoya. *Angew. Chem. Int. Ed.*, **44**, 2727 (2005).
[26] S.W. Lim, H. Moon, D. Kim, O.S. Jung. *Dalton Trans.*, **50**, 14320 (2021).
[27] M. Zhang, M.L. Saha, P.J. Stang. *Struct. Chem.*, **28**, 453 (2017).
[28] M. Kieffer, R.A. Bilbeisi, J.D. Thoburn, J.K. Clegg, J.R. Nitschke. *Angew. Chem. Int. Ed.*, **59**, 11369 (2020).
[29] A.R. Stefankiewicz, J.K.M. Sanders. *Chem. Commun.* , **49**, 5820 (2013).
[30] R.A. Bilbeisi, J.K. Clegg, N. Elgrishi, X. de Hatten, M. Devillard, B. Breiner, P. Mal, J.R. Nitschke. *J. Am. Chem. Soc.*, **134**, 5110 (2012).
[31] S. Zarra, J.K. Clegg, J.R. Nitschke. *Angew. Chem. Int. Ed.*, **52**, 4837 (2013).
[32] A. Stephenson, S.P. Argent, T. Riis-Johannessen, I.S. Tidmarsh, M.D. Ward. *J. Am. Chem. Soc.*, **133**, 858 (2011).
[33] S. Tashiro, M. Tominaga, T. Kusukawa, M. Kawano, S. Sakamoto, K. Yamaguchi, M. Fujita. *Angew. Chem. Int. Ed.*, **42**, 3267 (2003).
[34] Z. Xiao, H.F. Drake, Y.H. Rezenom, P. Cai, H.-C. Zhou. *Small Struct.*, **3**, 2100133 (2022). https://doi.org/10.1002/SSTR.202100133.
[35] E.J. Gosselin, G.E. Decker, B.W. McNichols, J.E. Baumann, G.P.A. Yap, A. Sellinger, E.D. Bloch. *Chem. Mater.*, **32**, 5872 (2020).
[36] C.R.K. Glasson, G.V. Meehan, C.A. Motti, J.K. Clegg, P. Turner, P. Jensen, L.F. Lindoy. *Dalton Trans.*, **40**, 10481 (2011).

[37] M.J. Burke, G.S. Nichol, P.J. Lusby. *J. Am. Chem. Soc.*, **138**, 9308 (2016).
[38] R.G. Siddique, K.S.A. Arachchige, H.A. Al-Fayaad, A.J. Brock, A.S. Micallef, E.T. Luis, J.D. Thoburn, J.C. McMurtrie, J.K. Clegg. *Chem. Commun.*, **57**, 4918 (2021).
[39] R.G. Siddique, K.S.A. Arachchige, H.A. AL-Fayaad, J.D. Thoburn, J.C. McMurtrie, J.K. Clegg. *Angew. Chem. Int. Ed.*, **61**, e202115555 (2022). https://doi.org/10.1002/ANGE.202115555.
[40] A.V. Davis, K.N. Raymond. *J. Am. Chem. Soc.*, **127**, 7912 (2005).
[41] D.L. Caulder, R.E. Powers, T.N. Parac, K.N. Raymond. *Angew. Chem. Int. Ed.*, **37**, 1840 (1998).
[42] A.J. Terpin, M. Ziegler, D.W. Johnson, K.N. Raymond. *Angew. Chem. Int. Ed.*, **40**, 157 (2001).
[43] C.M. Hong, M. Morimoto, E.A. Kapustin, N. Alzakhem, R.G. Bergman, K.N. Raymond, F.D. Toste. *J. Am. Chem. Soc.*, **140**, 6591 (2018).
[44] M.D. Pluth, R.G. Bergman, K.N. Raymond. *Acc. Chem. Res.*, **42**, 1650 (2009).
[45] D. Fiedler, D.H. Leung, R.G. Bergman, K.N. Raymond. *Acc Chem. Res.*, **38**, 349 (2005).
[46] M.D. Pluth, R.G. Bergman, K.N. Raymond. *Supramol. Catal.*, Chapter 7, **165**, (2008). https://doi.org/10.1002/9783527621781.ch7
[47] C.J. Brown, F.D. Toste, R.G. Bergman, K.N. Raymond. *Chem. Rev.*,**115**, 3012 (2015).
[48] M.D. Pluth, D.W. Johnson, G. Szigethy, A.V. Davis, S.J. Teat, A.G. Oliver, R.G. Bergman, K.N. Raymond. *Inorg. Chem.*, **48**, 111 (2009).
[49] G.R. Fulmer, A.J.M. Miller, N.H. Sherden, H.E. Gottlieb, A. Nudelman, B.M. Stoltz, J.E. Bercaw, K.I. Goldberg. *Organometallics*, **29**, 2176 (2010).
[50] C.G. Jones, M.W. Martynowycz, J. Hattne, T.J. Fulton, B.M. Stoltz, J.A. Rodriguez, H.M. Nelson, T. Gonen. *ACS Cent. Sci.*, **4**, 1587 (2018).